Published in final edited form as:
Cell Calcium. 2009 August ; 46(2): 114–121. doi:10.1016/j.ceca.2009.06.002.

Pathways of abnormal stress-induced Ca^{2+} influx into dystrophic *mdx* cardiomyocytes

M. Fanchaouy[a], **E. Polakova**[b], **C. Jung**[a], **J. Ogrodnik**[a], **N. Shirokova**[b], and **E. Niggli**[a]

[a]Department of Physiology, University of Bern, Buehlplatz 5, 3012 Bern, Switzerland [b]Department of Pharmacology & Physiology, UMDNJ - New Jersey Medical School, 185 S. Orange Ave., Newark 07103, NJ, USA.

Abstract

In Duchenne muscular dystrophy, deficiency of the cytoskeletal protein dystrophin leads to well-described defects in skeletal muscle, but also to dilated cardiomyopathy, accounting for about 20% of the mortality. Mechanisms leading to cardiomyocyte cell death and cardiomyopathy are not well understood. One hypothesis suggests that the lack of dystrophin leads to membrane instability during mechanical stress and to activation of Ca^{2+} entry pathways. Using cardiomyocytes isolated from dystrophic *mdx* mice we dissected the contribution of various putative Ca^{2+} influx pathways with pharmacological tools. Cytosolic Ca^{2+} and Na^{+} signals as well as uptake of membrane impermeant compounds were monitored with fluorescent indicators using confocal microscopy and photometry. Membrane stress was applied as moderate osmotic challenges while membrane current was quantified using the whole-cell patch-clamp technique. Our findings suggest a major contribution of two primary Ca^{2+} influx pathways, stretch-activated membrane channels and short-lived microruptures. Furthermore, we found evidence for a secondary Ca^{2+} influx pathway, the Na^{+}-Ca^{2+} exchange (NCX), which in cardiac muscle has a large transport capacity. After stress it contributes to Ca^{2+} entry in exchange for Na^{+} which had previously entered via primary stress-induced pathways, representing a previously not recognized mechanism contributing to subsequent cellular damage. This complexity needs to be considered when targeting abnormal Ca^{2+} influx as a treatment option for dystrophy.

1. Introduction

Duchenne muscular dystrophy (DMD) represents the most frequent dystrophy and affects 1 in approximately 4’000 male births. Mutations in the dystrophin gene on chromosome Xp21 result in the absence of a functional 427 kD protein dystrophin [1]. Dystrophin is a key element in the complex of proteins that connects the cytoskeleton to the extracellular matrix and its absence is thought to lead to mechanical instability of the cell membrane. However, progressive

Correspondence to: Ernst Niggli, Department of Physiology, University of Bern, Buehlplatz 5, 3012 Bern, Switzerland, P: +41 31 631-8730, F: +41 31 631-4611, E-mail: niggli@pyl.unibe.ch.

Conflict of interest
None declared.

degeneration and atrophy of skeletal muscle are not the only symptoms of DMD. Most patients also suffer from dystrophic cardiomyopathy, which is causal for 20% of the mortality [2].

Numerous cellular mechanisms contributing to the skeletal muscle pathology have been documented by using the dystrophic *mdx* mouse as a DMD model [3]. There seems to be a sequence of deleterious events which leads from a mechanical challenge to cellular injury and possibly cell death. The fragility of the sarcolemma is thought to result in abnormal stress-induced entry of Ca^{2+} into the cells and therefore to be responsible for the initial damage. However, the precise routes for this Ca^{2+} entry are not yet clear. Studies performed on dystrophic skeletal muscle suggest that most likely several pathways are involved (for review see [4]).

In cardiac muscle, similar cellular mechanisms are likely to be important for the initial damaging events in dystrophic cardiomyopathy. Previously we observed that mechanical stress mimicked by osmotic swelling generated abnormal SR Ca^{2+} release signals in *mdx* cardiomyocytes, such as Ca^{2+} waves and Ca^{2+} sparks. These signals were abolished in Ca^{2+} free solution, suggesting an involvement of transsarcolemmal Ca^{2+} influx in the initiation of abnormal SR Ca^{2+} release [5]. However, when *mdx* cells were treated with ryanodine and thapsigargin the Ca^{2+} responses were suppressed, confirming the SR as the main source of the Ca^{2+} signals. But under these conditions, small stress-induced elevations of [Ca^{2+}] were still detectable [5], suggesting that the extent of Ca^{2+} influx was rather small and that other mechanisms, such as the stress induced generation of reactive oxygen species (ROS), also contributed to the initiation of SR Ca^{2+} release signals.

In the present study, we explored the Ca^{2+} influx pathways contributing to stress-induced damage in *mdx* cardiomyocytes by recording the global Ca^{2+} signals that are amplified by SR Ca^{2+} release. We found that abnormal Ca^{2+} responses in *mdx* myocytes result from the parallel activation of multiple Ca^{2+} influx pathways, such as stretch-activated channels (SACs) and short-lived sarcolemmal microruptures. In addition, we identified Ca^{2+} entry mediated by Na^{+}-Ca^{2+} exchange (NCX) subsequent to Na^{+} entry via the other two pathways. This indirect mechanism for Ca^{2+} entry has not been previously considered to contribute to dystrophic muscle cell damage. Taken together, the combination of SACs, membrane microruptures and NCX provides additive pathways generating an abnormal rise of the Ca^{2+} concentration in response to membrane stretch, which is subsequently further amplified by Ca^{2+} induced Ca^{2+} release from the SR. Preliminary results of these studies have been published as an abstract [6].

2. Methods

2.1. Myocyte isolation

All animal procedures conformed with the *Guide for the Care and Use of Laboratory Animals* published by the US National Institutes of Health (NIH Publication No. 85-23, revised 1996) and were carried out with permission by local Swiss and U.S. authorities. C57BL/10 mice (5 – 10 months old), in the following referred to as wild-type (WT), and C57BL/10ScScn-*mdx* mice of identical age, were provided by Profs. M. Rüegg (University Basel, Switzerland) and U. Rüegg (University Geneva, Switzerland) or purchased from Jackson Laboratory. Ventricular myocytes were enzymatically isolated as previously described [7].

2.2. Solutions

Cells were perfused using a rapid superfusion system ($t_{1/2}$ for exchange < 0.5 s). The isotonic solution contained (in mM): 140 NaCl, 5.4 KCl, 1.8 $CaCl_2$, 1.1 $MgCl_2$, 5 HEPES, and 10

glucose, pH 7.4. The hypotonic solution contained (in mM): 70 NaCl, 5.4 KCl, 1.8 $CaCl_2$, 1.1 $MgCl_2$, 5 HEPES, and 10 glucose, pH 7.4. All experiments were carried out at 20°C.

2.3. Confocal imaging

Ca^{2+} imaging was performed on a laser-scanning confocal microscope (MRC-1000, Bio-Rad) with a 63×oil-immersion objective (Neofluar, 1.25 N.A.; Zeiss). Cells were loaded with fluo-3-AM (5 μM 30 min). Fluo-3 was excited at 488 nm with a semiconductor laser (Sapphire 488-10, Coherent), fluorescence was recorded above 515 nm. Amplitude (F/F_0) and time-course of Ca^{2+} transients were computed using Image SXM software [8].

Recording of Ca^{2+} signals in electrophysiological experiments was performed with a Yokogawa Nipkow scanner (Yokogawa) attached to a Zeiss Axiovert-200 microscope equipped with a 40 x, 1.2 N.A., water immersion objective (Zeiss). Cardiomyocytes were loaded with 50 μM K_5-fluo-3 *via* patch pipette. The 488 nm line of an argon ion laser (Laser Physics) was used to illuminate cells. Emission was recorded above 500 nm with a digital camera (MEGA 10X CCD with GENIII+ intensifier; Solamere) at 30 frames/s and then averaged over one second. Averaged values of intracellular fluorescence (F/F_0) were determined using ImageJ software (Wayne Rasband, NIH).

Changes in intracellular Na^+ concentration were followed with the sodium indicator SBFI (sodium-binding benzofuran isophthalate; 10 μM SBFI-AM, 90 min) and a RatioMaster M-40 photometer (PTI) mounted on a Zeiss Axiovert-200 microscope equipped with a quartz 40 x, 1.25 N.A., glycerol immersion objective (Partec). Cells were alternatingly illuminated at 340 and 380 nm at 1 Hz. Emission was collected above 500 nm, presented as excitation ratio and corrected with a linear function gained from baseline (2 min).

T-tubule structures and a possible detubulation in cardiomyocytes were evaluated by adding Di-8-ANEPPS after the osmotic swelling. In contrast, to assess membrane microruptures directly, osmotic stress was applied in a solution where 2.5 μM of the soluble membrane impermeable indicator FM1-43 was already present to allow for dye uptake via possible transient microruptures. The mean fluorescence 200 s after the stress normalized to the control fluorescence was averaged from 10 frames.

2.4. Electrophysiology

Currents were recorded in the whole-cell patch-clamp configuration using an Axopatch 200B amplifier (Axon). Patch electrodes (1.7 – 3 MΩ pulled from borosilicate glass were filled with (in mM): 120 K^+-aspartate, 5.5 $MgCl_2$, 8 NaCl, 20 HEPES, 5 K_2-ATP, 0.05 K_5-fluo-3 at 7.2 pH, adjusted with KOH. Whole-cell currents were measured at −70 mV while the external solution was briefly switched to hypotonic. The mean current difference was determined between the start and the end of the hypotonic superfusion.

2.5. Chemicals

Most chemicals were obtained from Sigma. Collagenase (type II) was purchased from Worthington, SBFI-AM from TefLabs, fluo-3 from Biotium and KB-R7943 from TOCRIS. GsMTx-4 was obtained from Prof. F. Sachs.

2.6. Statistics

Each set of data is expressed as a mean ± S.E.M. We employed Student's *t*-test to analyze data sets and significance is denoted as * ($P < 0.05$) or ** ($P < 0.02$).

3. Results

3.1. Osmotic swelling: a model of mechanical stress to trigger Ca^{2+} responses in resting *mdx* cardiomyocytes

Confocal imaging was used to record cytosolic Ca^{2+} transients in *mdx* cardiomyocytes loaded with fluo-3. Exchanging the isotonic (310 mOsm) to a moderately hypotonic solution (170 mOsm) for 30 s resulted in noticeable cell swelling, also visible as a dilution of the cytosolic fluo-3 signal. The Ca^{2+} responses elicited by this challenge were dependent on the cell type. Whereas resting *mdx* cardiomyocytes exhibited excessive cytosolic Ca^{2+} signals, such as bursts of Ca^{2+} sparks and repetitive Ca^{2+} waves (Fig. 1A-B), WT cells responded only moderately. In a recent study, we found that in dystrophic cells these excessive Ca^{2+} signals are ultimately driven by Ca^{2+}-induced Ca^{2+} release (CICR) from the SR [5]. However, they seemed to be triggered by transsarcolemmal Ca^{2+} influx, as Ca^{2+} free solution abolished them. Therefore, we explored possible stress-induced Ca^{2+} influx pathways in the present study. In the first series of experiments we analyzed the extent of these CICR signals as an indicator of Ca^{2+} influx, because stretch-induced Ca^{2+} influx itself was small and difficult to detect.

It is well known that long-lasting and strong osmotic shocks (15 minutes in 1500 mOsm) can lead to a disruption of the T-tubular system, resulting in detubulation [9,10]. For some of our experiments, this could represent a problem, particularly when the process of detubulation would cause a short-lived damage to the cell membrane. Therefore, we compared the T-tubule structure in cardiomyocytes by exposing the cells to Di-8-ANPPS either before or after an osmotic stress (Fig. 1C-D). These experiments revealed that the T-tubules remained accessible for Di-8-ANEPPS and therefore stayed connected to the extracellular space. The intact structure of the T-tubules suggests that the short and moderate cell swelling used in our experiments does not lead to detubulation of cardiomyocytes. Please note that these experiments would not detect dye entry into the cells via short-lived microruptures during the osmotic swelling, because Di-8-ANEPPS was not present during the swelling itself, only either before or after this maneuver. Therefore, the staining is only due to dye accumulation within the sarcolemmal membrane (see below for dye uptake experiments with FM1-43).

3.2. Membrane microruptures

Short-lived stress-induced membrane microruptures have been shown to occur in dystrophic skeletal muscle [11,12] and more recently also in cardiac muscle [13]. Microruptures of the sarcolemma are usually repaired within a few seconds [14], but the surfactant Poloxamer-188 has been found to either lead to more rapid repair or to entirely prevent membrane disruption through a direct interaction with the lipid bilayer [15].

We therefore used Poloxamer-188 as a tool to examine whether Ca^{2+} influx via membrane microruptures contributes to stress-induced Ca^{2+} responses. The application of 150 μM Poloxamer-188 prevented the abnormal Ca^{2+} signals (Fig. 2A). For statistical comparison between different groups of cells, we determined the normalized mean fluo-3 fluorescence (F/F_0) during 90 s after returning to the isotonic solution. In *mdx* cardiomyocytes under control conditions (no Poloxamer-188 added), the mean fluorescence increased from 1.00 to 1.30±0.13 F/F_0 (n=7) while it reached only 1.05±0.02 F/F_0 (n=7) in the presence of Poloxamer-188 (Fig. 2B). Even though the cells treated with the membrane sealant did not exhibit Ca^{2+} bursts, the fluo-3 fluorescence recorded after the stress still increased, albeit slowly, to about 14% above the initial value. This may arise from Ca^{2+} entry routes other than membrane microruptures. Due to its direct interaction with the cell membrane Poloxamer-188 is most likely not specific and may not only block Ca^{2+} entry through microruptures but also via other pathways, thereby making it difficult to exclusively attribute its actions to the existence of microruptures.

Therefore, the permeability of the sarcolemma was assessed more directly by quantifying cellular uptake of the lipophilic fluorescent indicator FM1-43 (2.5 μM), which, in contrast to the T-tubule staining experiments above, was present in the extracellular solution during the osmotic stress [16]. This dye can enter the cytosolic space only through sarcolemmal microruptures, but is too large to pass via any of the other putative Ca^{2+} influx pathways, such as SACs. Initially, we compared the stress-induced uptake of FM1-43 between WT and *mdx* myocytes (Figs. 2C and 2D). The normalized fluorescence increase after stress was significantly higher in the *mdx* cardiomyocytes (34.1±3.9%; n=23) than in the WT cardiomyocytes (19.4±2.0%; n=18). Moreover, visualization of the dye entry into the cytoplasm of *mdx* myocytes often revealed fluorescent regions in proximity to the sarcolemma (Fig. 2Cb, center). This was even more evident in calculated images representing dye uptake as the difference of fluorescence before and after the osmotic challenge was applied (Fig. 2Cc, center). Addition of Poloxamer-188 also reduced stress-induced FM1-43 uptake in *mdx* myocytes to levels comparable to WT cells (fluorescence increase 15.1±2.8% (n=13). The fluorescence increase observed in WT cells most likely does not represent cytosolic accumulation over time, but rather binding to the superficial and T-tubular sarcolemma. Taken together, these findings indicate that short-lived stress-induced microruptures indeed occur in *mdx* cardiomyocytes and that they may contribute to the trigger for excessive intracellular Ca^{2+} responses.

3.3. Stretch- activated channels (SACs)

SACs are permeable to Na^+, K^+, and to Ca^{2+} [17]. These mechanosensitive ion channels have been proposed to be one of the pathways for stress-induced Ca^{2+} entry in dystrophic skeletal and cardiac muscle [4,18]. In the present study, we applied several inhibitors of SACs, to evaluate their possible contribution to stress-induced SR Ca^{2+} release signals.

Gadolinium ions (Gd^{3+}) are unspecific inhibitors of different membrane currents [19,20] and are believed to interfere with the SACs. Under control conditions, mechanical stress stimulated *mdx* myocytes to produce substantial Ca^{2+} signals (Fig. 3A). Addition of 10 μM Gd^+ significantly decreased the amplitude of these Ca^{2+} responses. The average level of fluo-3 fluorescence recorded during the first 90 s after returning to the isotonic solution was significantly reduced from 1.37±0.02 F/F_0 (n=11) to 1.12±0.01 F/F_0 (n=10) in myocytes exposed to Gd^{3+} (Fig. 3D).

This suppression of the stress-induced Ca^{2+} signals is consistent with a block of SACs but could also arise from a less specific action of Gd^{3+}. Instead of testing various concentrations of Gd^{3+}, we carried out two experimental series using streptomycin and GsMTx-4. The aminoglycoside antibiotic streptomycin has been reported to be a somewhat more specific inhibitor of the SACs and to reduce Ca^{2+} leak influx in resting muscle [18]. The most specific inhibitor for SACs available today is the tarantula spider toxin GsMTx-4 [21]. Preincubation (10 min) in 100 μM streptomycin significantly reduced intracellular Ca^{2+} responses in *mdx* cardiomyocytes (Fig. 3B). The average fluorescence after the stress decreased from 1.22±0.12 F/F_0 (n=8) to 1.01±0.07 F/F_0 (n=14) in the presence of streptomycin (Fig. 3D). Likewise, 5 μM GsMTx-4 reduced the Ca^{2+} responses from 1.28±0.06 F/F_0 (n=19) to 1.08±0.03 F/F_0 (n=14) (Fig. 3D). Taken together, Gd^{3+}, streptomycin and GsMTx-4 significantly suppressed the signals induced by osmotic stress, suggesting that stretch-activated membrane channels may also contribute to the stress-induced Ca^{2+} load.

3.4. Ionic inward currents and quantification of block by Poloxamer-188 and streptomycin

In a previous study we found that the changes of the average cytosolic Ca^{2+} concentration due to Ca^{2+} entry into cells in response to osmotic stress were rather small [5]. Therefore, here we

used a more sensitive and more quantitative electrophysiological method to directly measure stress-induced ion fluxes.

Cells were voltage clamped and held at −70 mV while whole-cell currents were recorded during and after osmotic stress. Representative traces are A*b* and A*d* in Fig. 4A. Traces A*a* and A*c* show corresponding intracellular Ca^{2+} signals. The inward current activated by stress in *mdx* myocytes was significantly larger than in WT cells (421.4 ± 46.9 pA, n=18 vs 80.2 ± 23.9 pA, n=15) (Fig. 4B).

Next we examined whether and to what extent Poloxamer-188 and streptomycin (the drugs we used in previous experiments to test the role of transient microruptures and SACs) affect the stress-induced ionic currents. In agreement with and confirming the results illustrated in Figs. 2 and 3, both drugs significantly reduced the inward currents. Compared to untreated cells they were inhibited by ~80 % (to 150.9 ± 53.3 pA, n=11) and by ~75 % (to 163.8 ± 33.6, n=11) in the presence 150 μM Poloxamer-188 and 100 μM streptomycin, respectively (Fig. 4B).

These electrophysiological data provide further support for the notion that both, membrane microruptures and SACs, contribute to the membrane leak and ionic current in dystrophic cardiomyocytes. These two pathways are not ion specific and the inward current is likely to reflect not only Ca^{2+} influx. Given that Na^+ is the main extracellular ion and both pathways are highly permeable to Na^+, a substantial fraction of the stretch-induced inward current is presumably carried by Na^+. Therefore, we attempted to evaluate the magnitude of Na^+ influx. For this, we examined changes in intracellular [Na^+] which may result from the Na^+ entry into the cell following osmotic challenges. Myocytes were loaded with the ratiometric Na^+ indicator SBFI and the fluorescence ratio was quantified with photometry. Fig. 4C illustrates representative Na^+ signals in *mdx* and WT cells that were subjected to stress. After an initial reduction of $[Na^+]_i$ due to dilution of the cytosol by entering water, the Na^+ signals recovered upon return to isotonic solution but then slowly increased above the level recorded before the osmotic stress. In respect to the base line levels, the increase was significant and almost five times larger in *mdx* than in WT myocytes (0.0055 ± 0.00069 F_{380}/F_{340} (n=18) vs 0.00146 ± 0.00042 F_{380}/F_{340} (n=16) in *mdx* and WT respectively), indicating larger changes in $[Na^+]_i$ and most likely larger Na^+ influx in *mdx* cells.

3.5. Role of the NCX

Na^+ which entered the cytosol through membrane microruptures and SACs could interact with the NCX, which is highly expressed and has a large Ca^{2+} transport capacity in cardiomyocytes. This in turn might lead to Ca^{2+} entry via activation of the NCX reverse mode to remove the previously entered Na^+.

To test for an involvement of the reverse mode NCX, we applied several NCX inhibitors. Acute addition of 5 mM Ni^{2+}, a widely used but not specific NCX inhibitor, indeed prevented the abnormal Ca^{2+} responses to osmotic stress in *mdx* cardiomyocytes (Fig. 5A,C). Similarly, 20 μM KB-R7943 led to a decrease of the Ca^{2+} response, suggesting that the NCX indeed contributes to Ca^{2+} entry. Both, Ni^{2+} and KB-R7943 can also interfere with the voltage-activated L-type Ca^{2+} channels. However, the extent of membrane depolarization during and after the osmotic challenge was found to be only a few millivolts (data not shown), insufficient to activate L-type Ca^{2+} current.

Interestingly, subsequent to the removal of Ni^{2+} (or KB-R7943) a few minutes after the osmotic stress, Ca^{2+} responses reappeared in 46% of *mdx* cells with a delay (see Fig. 5D for representative examples). These delayed signals were presumably triggered by Ca^{2+} driven into the cells by reverse mode of the NCX, which became active again after washout of the NCX inhibitors. In other words, it could arise after the initial intracellular accumulation of

Na^+ via microruptures and SACs as described above. Accumulated Na^+ then becomes exchanged for Ca^{2+} by the NCX after relief of its inhibition.

Taken together, these observations suggest that in dystrophic cardiomyocytes stretch-activated channels, membrane microruptures and the NCX in additively contribute to Ca^{2+} influx triggering abnormal Ca^{2+} signals in response to membrane stretch.

4. Discussion

4.1. Primary stress-activated influx pathways

The membrane fragility hypothesis of dystrophic muscle is based on a broad foundation of experimental evidence. It is widely accepted that mechanical stress leads to abnormal "leakiness" of the sarcolemma. In this context, it is believed that entry of Ca^{2+} represents an important component for the cellular injury subsequent to membrane damage. However, the exact mechanisms and pathways by which the membrane damage and influx of Ca^{2+} occurs are much less clear, even in skeletal muscle, where most of these studies have been carried out. Despite numerous attempts to identify stress-induced Ca^{2+} influx pathways, the picture has remained confusing [4]. Part of the problem lies in the fact that the methods available for this type of studies are less than perfect. Lack of specific pharmacological tools represents a major experimental difficulty, but also the fact that the molecular entities of candidate channels are not yet known. However, some TRP channel subunits have been proposed to be part of stretch-activated channels [22] and TRPC1 was found to be overexpressed in dystrophic cardiac myocytes [23].

Despite these difficulties known from experimental work on skeletal muscle, we made an attempt to identify some of the Ca^{2+} influx pathways involved in dystrophic cardiomyopathy, because each of them might be a promising pharmacological target for strategies aimed at slowing down disease progression. Notably, the cardiac manifestations of muscle dystrophy have only recently received the deserved attention with research studies and the mechanisms involved in this pathology are still largely unknown.

Membrane stretch by mild and brief hypo-osmotic swelling has been used successfully in several recent studies [5,24,25]. However, longer exposure to strong osmotic shocks is known to detach the T-tubules and essentially de-tubulate skeletal and cardiac muscle [10,26]. The process of detubulation would cause damage to the cell membrane and then could represent a problem, particularly for the evaluation of microruptures in the sarcolemma. Since we did not know *a priori* that detubulation did not occur during our experiments with mild and brief osmotic challenges, we carried out initial experiments to ensure that detubulation was not a problem. We found that even after the osmotic challenge the T-tubules remained fully accessible to the extracellularly applied lipophilic fluorescent indicator Di-8-ANEPPS, confirming that detubulation did not occur in our experiments.

Classical stretch-activated Ca^{2+} influx pathways that have previously been considered in skeletal muscle include the stretch-activated channels (SACs) [27], which were proposed to be abnormally stress-sensitive in dystrophy. Our experiments support the notion that SACs are involved in the abnormal response of dystrophic *mdx* myocytes to osmotic challenges. The evidence is based on the combination of three inhibitors. Gd^{3+} is a very unspecific SAC blocker and may interfere with other possible Ca^{2+} entry pathways, even at low concentrations (e.g. Ca^{2+} channels [19,20]). Therefore, we also carried out a series of experiments with streptomycin, which is thought to be somewhat more specific for SACs [28]., But also this compound has been reported to interfere with diverse Ca^{2+} channels, not only stretch activated channels [29]. Finally, the most specific inhibitor known today, the tarantula toxin GsMTx-4, was also found to reduce the signals, although not completely. Taken together, these findings

suggest that Ca^{2+} influx pathways other than SACs are present as well, which are unspecifically blocked by Gd^{3+} and streptomycin, but not by the most specific GsMTx-4.

The involvement of another pathway has been invoked in damage of dystrophic skeletal muscle, particularly after eccentric stretch. Short-lived microruptures of the cell membrane were proposed to be present, although it is not yet clear whether they occur as a primary event or with a delay subsequent to Ca^{2+} entry. The surfactant Poloxamer-188 is used in cell culture media because it lowers the sensitivity of cells towards shear stress [30]. This compound is thought to prevent or rapidly re-seal membrane microruptures [31] and was found to protect the heart of dystrophic mice [13]. To assess whether membrane microruptures may be involved in the stress-induced Ca^{2+} signals in our study, we carried out an experimental series with *mdx* cardiomyocytes in the presence and absence of Poloxamer-188. The results indicate that Poloxamer-188 indeed protected the cells from the damage, but again we were faced with the problem that this compound is unlikely to be a specific inhibitor of microruptures and could also block other pathways. Since the microruptures have a much larger pore opening than membrane ion channels, fluorescent molecules which cannot pass membrane channels could still permeate the microruptures. Thus, we investigated the uptake of the fluorescent indicator FM1-43. This lipophilic dye does not permeate into intact cells and has previously been used to quantify synaptic vesicle cycling activity and membrane repair [32].

Our confocal imaging experiments revealed that FM1-43 uptake into the cytosol during stress was significant only in *mdx* cells. This is particularly visible in the calculated difference images. The uptake appeared to be quite patchy with regions of high fluorescence under the sarcolemma, presumably located near regions where microruptures had occurred. Inside the cell, the dye did not diffuse rapidly, probably because of its lipophilicity and the presence of many organelles with membranes (e.g. mitochondria, SR). The fluorescence in WT cells mostly corresponded to dye which had accumulated and could not be washed out from the T-tubules and cell membrane, and was thus not related to uptake into the cytosol. Interestingly, addition of Poloxamer-188 completely prevented the internalization of FM1-43 in *mdx* myocytes, confirming that the main benefit of Poloxamer-188 is mediated by its membrane sealing properties. Taken together, our observations indicate that SACs and membrane microruptures play important roles as primary stretch-activated leak pathways in *mdx* dystrophic cardiomyocytes.

4.2. Secondary Ca^{2+} influx pathways: role of reverse mode NCX

The ionic influx pathways mentioned so far, SACs and microruptures, are thought to be opened by mechanical stress, allowing extracellular Ca^{2+} to enter the cytosol. However, both pathways are unspecific and will allow other ions to enter, most importantly Na^+. The influx we measured as stress-induced membrane current under voltage-clamp conditions most likely resulted mainly from Na^+ entry. While this may cause little harm in skeletal muscle, the situation is likely to be different in cardiac muscle because in this tissue the NCX is highly expressed and is very active. Normally, the NCX is responsible for the beat-to-beat removal of Ca^{2+} which had entered the cell on I_{Ca}. But depending on the electrochemical gradients for Na^+ and Ca^{2+} the NCX can also work in a Ca^{2+} influx mode. Entry of Na^+ via the aforementioned direct influx pathways may lead to an accumulation of intracellular Na^+, which in turn would drive the NCX into the Ca^{2+} influx mode. This scenario was supported in our study by several findings. First of all, inhibiting the NCX with Ni^{2+} or KB-R7943 suppressed the abnormal Ca^{2+} signals in *mdx* cardiomyocytes, suggesting an important contribution of the Ca^{2+} influx via the NCX. KB-R7943 is an inhibitor preferentially blocking the Ca^{2+} influx mode of the NCX. At 20 μM it was shown to inhibit 80% of $^{45}Ca^{2+}$ uptake [33]. At such concentrations it would also block the L-type Ca^{2+} channels. However, the osmotic shock only led to a very slight depolarisation of the cells (from approximately −80 mV to around −78 mV, data not

shown), making an activation of these channels, and therefore this unwanted side-effect, unlikely. In addition, using the Na^+ indicator SBFI we indeed detected a small elevation of $[Na^+]_i$ in *mdx* myocytes. Assuming a resting $[Na]_i$ of 8 mM, we estimated the increase of the global $[Na]_i$ in *mdx* myocytes to be around 350 μM, because we know from our previous study that the dilution of the cytosol at the end of the hypo-osmotic period is very reproducible and amounts to 15.8% [5]. Please note that even small fractional changes of the global cellular Na^+ concentration already correspond to substantial fluxes, as the concentrations are in the millimolar range. In addition, Na^+ may reach higher than average cytosolic concentrations underneath the sarcolemma, which will be relevant for the NCX [34–36]. Yet another observation is in line with a functional role for some Na^+ accumulation. Removal of the NCX inhibitors at the end of the experiment (and thus rapid unblock of the NCX) was often followed by the appearance and rebound of abnormal Ca^{2+} signals. This suggests that stressed myocytes can exhibit quite prolonged Na^+ influx which would maintain elevated Na^+ concentrations until the NCX inhibitor is removed, leading to a re-activation of NCX in its Ca^{2+} influx mode. To what extent each of the pathways finally contributes to the total entry of Ca^{2+} will depend on many factors (e.g. the electrochemical driving forces, the buffering and diffusion of Na^+ and Ca^{2+} in the submembrane space, the density and activity of the involved transporters and channels, etc.). In any case, it appears that the NCX plays an important role in cardiac muscle.

Taken together our findings indicate that in dystrophic cardiomyocytes several Ca^{2+} influx pathways act in parallel and additively contribute to abnormal stress-induced Ca^{2+} entry. While we have compelling evidence for an involvement of SACs, microruptures and the NCX, we cannot exclude the participation of other pathways, such as leak-channels and SOCs. As one might expect, the contribution of the various pathways to the damaging Ca^{2+} entry is additive. Therefore, interfering with one or the other can be sufficient to bring the total Ca^{2+} entry below the threshold for the generation of excessive SR Ca^{2+} release signals. Nevertheless, for future pharmacological strategies attempting to reduce stress-induced Ca^{2+} entry in dystrophy, our findings would suggest that preferably several pathways should be targeted simultaneously.

Acknowledgements

This work was supported by the Swiss Foundation for Research on Muscle Diseases [to E.N.&N.S.]; National Institutes of Health [AR053933 to N.S.], Swiss National Science Foundation [31-109693.05 to E.N.]; Muscular Dystrophy Association [to N.S.]; American Heart Association [to N.S.]; UMDNJ foundation [to N.S.] and Sigrist Foundation [to E.N.&N.S]. We thank Fred Sachs for GsMTx-4 and Daniel Lüthi for technical assistance.

References

1. Ervasti JM, Campbell KP. Dystrophin and the membrane skeleton. Curr Opin Cell Biol 1993;5:82–87. [PubMed: 8448034]
2. Finsterer J, Stollberger C. The heart in human dystrophinopathies. Cardiology 2003;99:1–19. [PubMed: 12589117]
3. Quinlan JG, Hahn HS, Wong BL, Lorenz JN, Wenisch AS, Levin LS. Evolution of the *mdx* mouse cardiomyopathy: physiological and morphological findings. Neuromuscul Disord 2004;14:491–496. [PubMed: 15336690]
4. Allen DG, Whitehead NP, Yeung EW. Mechanisms of stretch-induced muscle damage in normal and dystrophic muscle: role of ionic changes. J Physiol 2005;567:723–735. [PubMed: 16002444]
5. Jung C, Martins AS, Niggli E, Shirokova N. Dystrophic cardiomyopathy: amplification of cellular damage by Ca^{2+} signalling and reactive oxygen species-generating pathways. Cardiovasc Res 2008;77:766–773. [PubMed: 18056762]
6. Fanchaouy M, Polakova E, Jung C, Ogrodnik J, Shirokova N, Niggli E. Pathways of abnormal stress-induced calcium influx into dystrophic *mdx* cardiomyocytes. Biophysical Journal 2009;96:274a.
7. Wolska BM, Solaro RJ. Method for isolation of adult mouse cardiac myocytes for studies of contraction and microfluorimetry. Am J Physiol 1996;271:H1250–H1255. [PubMed: 8853365]

8. Barrett SD. Software for scanning microscopy. Proc Royal Microscop Soc 2002;37:167–174.
9. Kawai M, Hussain M, Orchard CH. Excitation-contraction coupling in rat ventricular myocytes after formamide-induced detubulation. Am J Physiol 1999;277:H603–H609. [PubMed: 10444485]
10. Swift F, Tovsrud N, Enger UH, Sjaastad I, Sejersted OM. The Na^+/K^+-ATPase alpha2-isoform regulates cardiac contractility in rat cardiomyocytes. Cardiovasc Res 2007;75:109–117. [PubMed: 17442282]
11. McNeil PL, Khakee R. Disruptions of muscle fiber plasma membranes. Role in exercise-induced damage. Am J Pathol 1992;140:1097–1109. [PubMed: 1374591]
12. Petrof BJ, Shrager JB, Stedman HH, Kelly AM, Sweeney HL. Dystrophin protects the sarcolemma from stresses developed during muscle contraction. Proc Natl Acad Sci U S A 1993;90:3710–3714. [PubMed: 8475120]
13. Yasuda S, Townsend D, Michele DE, Favre EG, Day SM, Metzger JM. Dystrophic heart failure blocked by membrane sealant poloxamer. Nature 2005;436:1025–1029. [PubMed: 16025101]
14. Cai C, Masumiya H, Weisleder N, Matsuda N, Nishi M, Hwang M, Ko JK, Lin P, Thornton A, Zhao X, Pan Z, Komazaki S, Brotto M, Takeshima H, Ma J. MG53 nucleates assembly of cell membrane repair machinery. Nat Cell Biol 2009;11:56–64. [PubMed: 19043407]
15. Maskarinec SA, Hannig J, Lee RC, Lee KY. Direct observation of poloxamer 188 insertion into lipid monolayers. Biophys J 2002;82:1453–1459. [PubMed: 11867460]
16. Togo T, Alderton JM, Bi GQ, Steinhardt RA. The mechanism of facilitated cell membrane resealing. J Cell Sci 1999;112:719–731. [PubMed: 9973606]
17. Hu H, Sachs F. Stretch-activated ion channels in the heart. J Mol Cell Cardiol 1997;29:1511–1523. [PubMed: 9220338]
18. Ward ML, Williams IA, Chu Y, Cooper PJ, Ju YK, Allen DG. Stretch-activated channels in the heart: contributions to length-dependence and to cardiomyopathy. Prog Biophys Mol Biol 2008;97:232–249. [PubMed: 18367238]
19. Lacampagne A, Gannier F, Argibay J, Garnier D, Le Guennec JY. The stretch-activated ion channel blocker gadolinium also blocks L-type calcium channels in isolated ventricular myocytes of the guinea-pig. Biochim Biophys Acta 1994;1191:205–208. [PubMed: 8155676]
20. Babich O, Matveev V, Harris AL, Shirokov R. Ca^{2+}-dependent inactivation of $Ca_V1.2$ channels prevents Gd^{3+} block: does Ca^{2+} block the pore of inactivated channels? J Gen Physiol 2007;129:477–483. [PubMed: 17535960]
21. Suchyna TM, Johnson JH, Hamer K, Leykam JF, Gage DA, Clemo HF, Baumgarten CM, Sachs F. Identification of a peptide toxin from Grammostola spatulata spider venom that blocks cation-selective stretch-activated channels. J Gen Physiol 2000;115:583–598. [PubMed: 10779316]
22. Dyachenko V, Husse B, Rueckschloss U, Isenberg G. Mechanical deformation of ventricular myocytes modulates both TRPC6 and Kir2.3 channels. Cell Calcium 2009;45:38–54. [PubMed: 18635261]
23. Williams IA, Allen DG. Intracellular calcium handling in ventricular myocytes from *mdx* mice. Am J Physiol Heart Circ Physiol 2007;292:H846–H855. [PubMed: 17012353]
24. Wang X, Weisleder N, Collet C, Zhou J, Chu Y, Hirata Y, Zhao X, Pan Z, Brotto M, Cheng H, Ma J. Uncontrolled calcium sparks act as a dystrophic signal for mammalian skeletal muscle. Nat Cell Biol 2005;7:525–530. [PubMed: 15834406]
25. Martins AS, Shkryl VM, Nowycky MC, Shirokova N. Reactive oxygen species contribute to Ca^{2+} signals produced by osmotic stress in mouse skeletal muscle fibres. J Physiol 2008;586:197–210. [PubMed: 17974587]
26. Koutsis G, Philippides A, Huang CL. The afterdepolarization in Rana temporaria muscle fibres following osmotic shock. J Muscle Res Cell Motil 1995;16:519–528. [PubMed: 8567939]
27. Suchyna TM, Sachs F. Mechanosensitive channel properties and membrane mechanics in mouse dystrophic myotubes. J Physiol 2007;581:369–387. [PubMed: 17255168]
28. Iribe G, Kohl P. Axial stretch enhances sarcoplasmic reticulum Ca^{2+} leak and cellular Ca^{2+} reuptake in guinea pig ventricular myocytes: experiments and models. Prog Biophys Mol Biol 2008;97:298–311. [PubMed: 18395247]
29. Parsons TD, Obaid AL, Salzberg BM. Aminoglycoside antibiotics block voltage-dependent calcium channels in intact vertebrate nerve terminals. J Gen Physiol 1992;99:491–504. [PubMed: 1317913]

30. Palomares LA, Gonzalez M, Ramirez OT. Evidence of Pluronic F-68 direct interaction with insect cells: impact on shear protection, recombinant protein, and baculovirus production. Enzyme Microb Technol 2000;26:324–331. [PubMed: 10713203]

31. Sharma V, Stebe K, Murphy JC, Tung L. Poloxamer 188 decreases susceptibility of artificial lipid membranes to electroporation. Biophys J 1996;71:3229–3241. [PubMed: 8968593]

32. Cai C, Masumiya H, Weisleder N, Matsuda N, Nishi M, Hwang M, Ko JK, Lin P, Thornton A, Zhao X, Pan Z, Komazaki S, Brotto M, Takeshima H, Ma J. MG53 nucleates assembly of cell membrane repair machinery. Nat Cell Biol 2008;11:56–64. [PubMed: 19043407]

33. Iwamoto T, Watano T, Shigekawa M. A novel isothiourea derivative selectively inhibits the reverse mode of Na+/Ca2+ exchange in cells expressing NCX1. J Biol Chem 1996;271:22391–22397. [PubMed: 8798401]

34. Lederer WJ, Niggli E, Hadley RW. Sodium-calcium exchange in excitable cells: fuzzy space. Science 1990;248:283. [PubMed: 2326638]

35. Hirn C, Shapovalov G, Petermann O, Roulet E, Ruegg UT. $Na_V1.4$ deregulation in dystrophic skeletal muscle leads to Na^+ overload and enhanced cell death. J Gen Physiol 2008;132:199–208. [PubMed: 18625851]

36. Gavillet B, Rougier JS, Domenighetti AA, Behar R, Boixel C, Ruchat P, Lehr HA, Pedrazzini T, Abriel H. Cardiac sodium channel $Na_V1.5$ is regulated by a multiprotein complex composed of syntrophins and dystrophin. Circ Res 2006;99:407–414. [PubMed: 16857961]

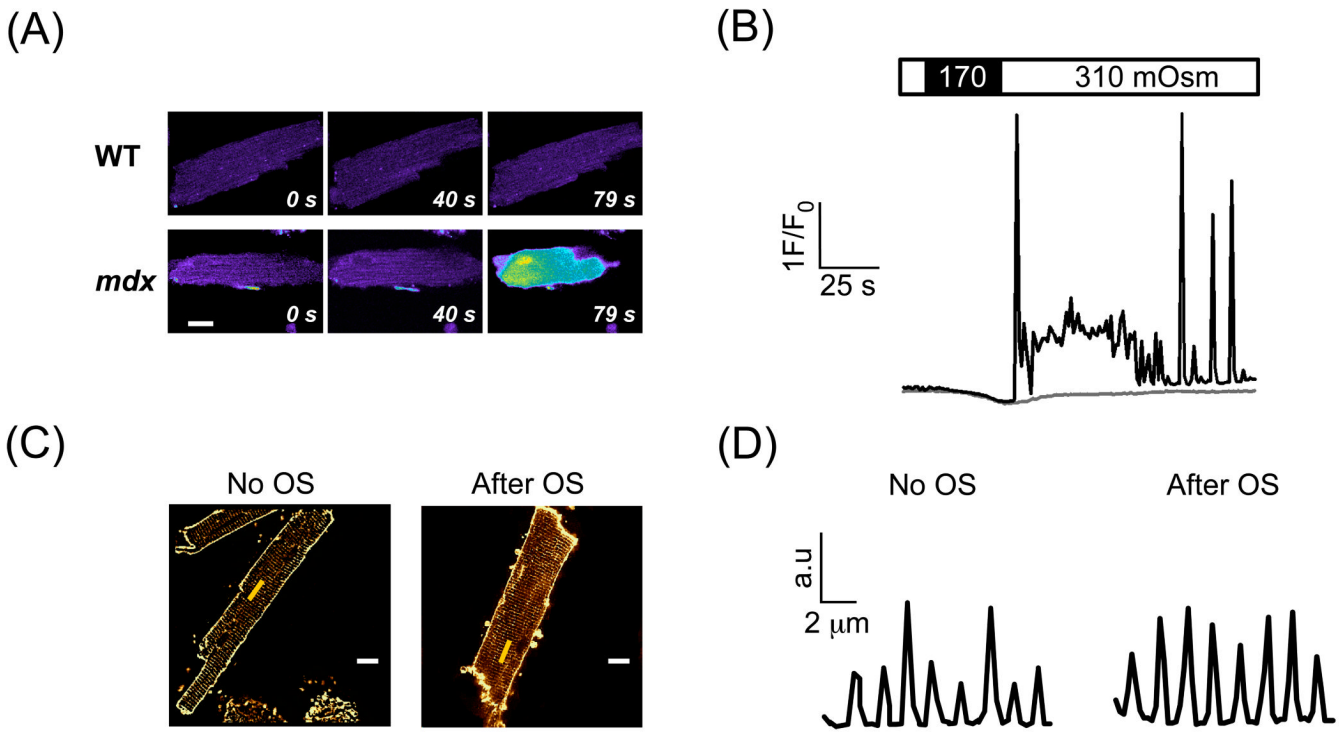

Fig. 1.

Stress-induced intracellular Ca^{2+} signals in *mdx* cardiac myocytes loaded with fluo-3. (*A*) Confocal fluorescence images of Ca^{2+} signals in response to an osmotic challenge in WT and *mdx* myocytes. (*B*) Exposure to low osmolarity stimulates SR Ca^{2+}-release signals. Traces represent normalized fluorescence signals in an *mdx* (black trace) and WT cardiomyocyte (grey trace). (*C*) Cell membrane of WT myocytes was stained with 5 μM Di-8-ANEPPS either in control conditions or after recovery from osmotic stress (OS). White scale bars: 10 μm. The yellow line indicates the region for the profile in (*D*). Pattern of T-tubule fluorescence in control (left panel) and after stress (right panel). Sarcomere length was around 2 μm in both cells.

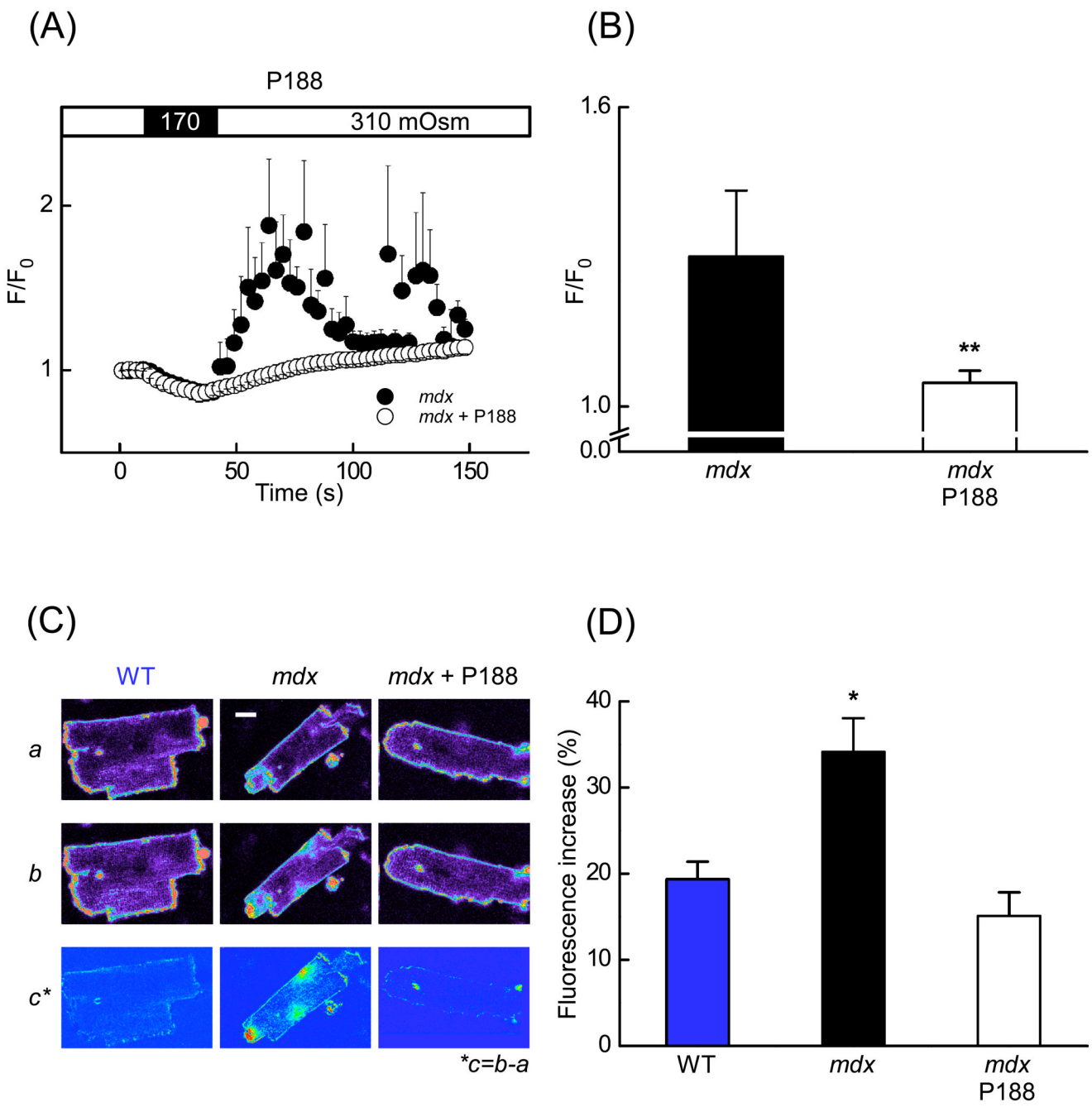

Fig. 2.

Poloxamer-188 (P-188) abolished stress-induced Ca^{2+} signals and prevented membrane microruptures in *mdx* cardiac myocytes. (*A*) Time-course of normalized fluorescence from fluo-3 in *mdx* myocytes (black circles) (n = 7 cells) and in *mdx* cells pretreated with 150 μM P-188 (white circles) (n = 7 cells). (*B*) Mean Ca^{2+} related fluorescence of cardiomyocytes recorded during 90 s after the osmotic challenge (from *A*) in control *mdx* (black bar) and *mdx* cells pretreated with P-188 (white bar). (*C*) Fluorescence images of cardiomyocytes continuously perfused with the lipophilic dye FM1-43 (2.4 μM) to detect transient membrane microruptures. The first images (Ca) were obtained before the stress. The second row of images (Cb) were captured 160 s after the osmotic challenge. Experiments were carried out with WT

myocytes, *mdx* cells under control conditions and in the presence of 150 μM P-188. The bottom row of images (Cc) represents the difference (b – a). (*D*) Statistical analysis of the data as the fluorescence increase measured over the entire area of cardiomyocytes in WT, *mdx* and *mdx* cells pretreated with 150 μM P-188 (n = 18 cells for WT, n = 23 cells for *mdx* control, n = 13 cells for *mdx* with P188). Scale bars: 10 μm.

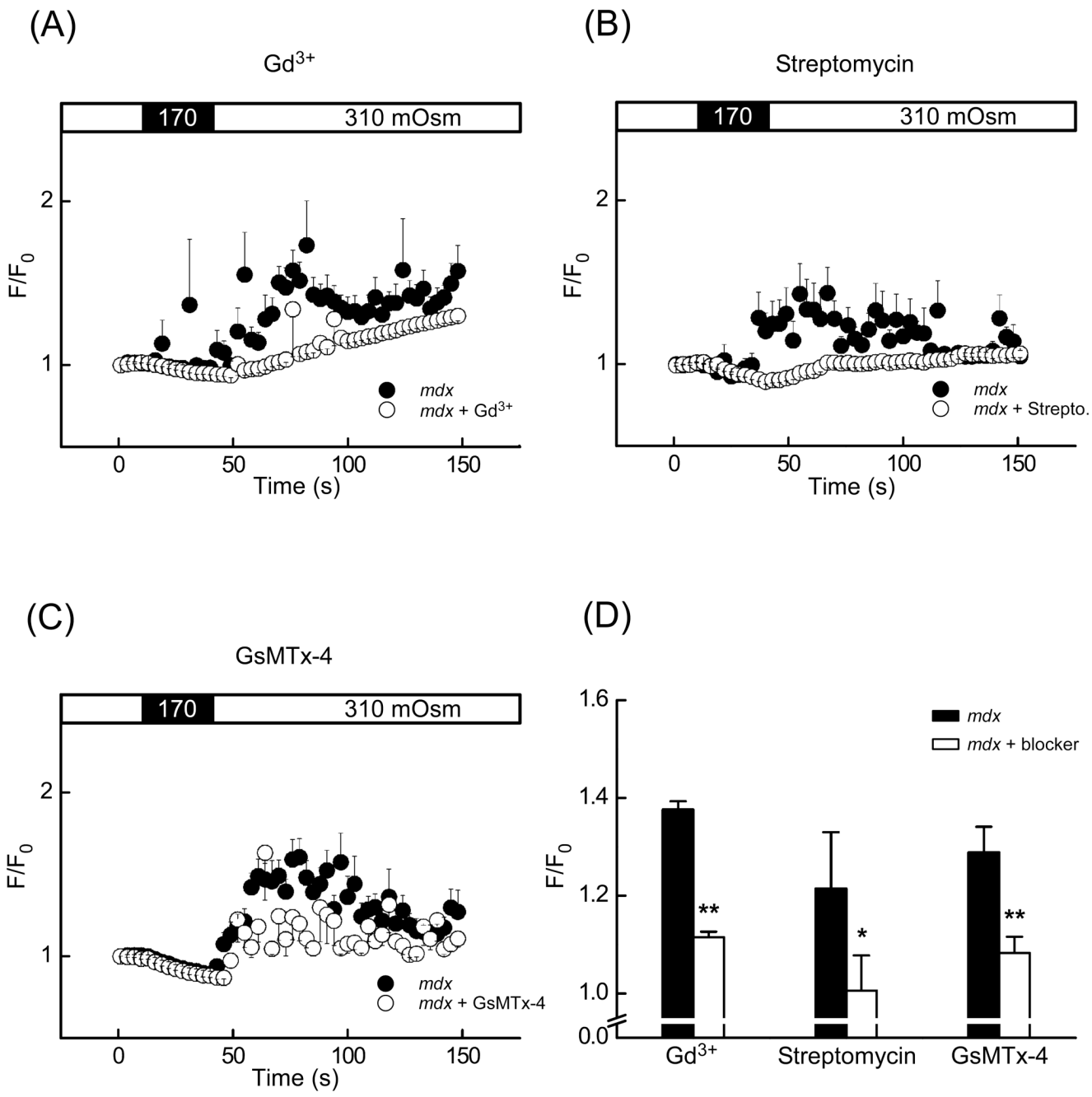

Fig. 3.

Stretch-activated channel inhibitors Gd^{3+}, streptomycin and GsMTx-4 significantly decreased the amplitude of stress-induced intracellular Ca^{2+} signals in *mdx* cardiomyocytes loaded with fluo-3. (*A*–*C*) Time-course of normalized fluorescence in *mdx* cells in control solution (black circle) and in *mdx* pretreated with an inhibitor (white circle). (*A*) Superfusion with 10 μM Gd^{3+}, (B) with 100 μM streptomycin (*C*) with 5 μM GsMTx-4. (*D*) Mean fluorescence intensity 90 s after the application of stress in *mdx* cardiomyocytes (white bar) and *mdx* cardiomyocytes pretreated with an inhibitor (black bar) (number of cells was n = 11, 8, 19 for controls, n = 10, 14, 14 for Gd^{3+}, streptomycin and GsMTx-4, respectively).

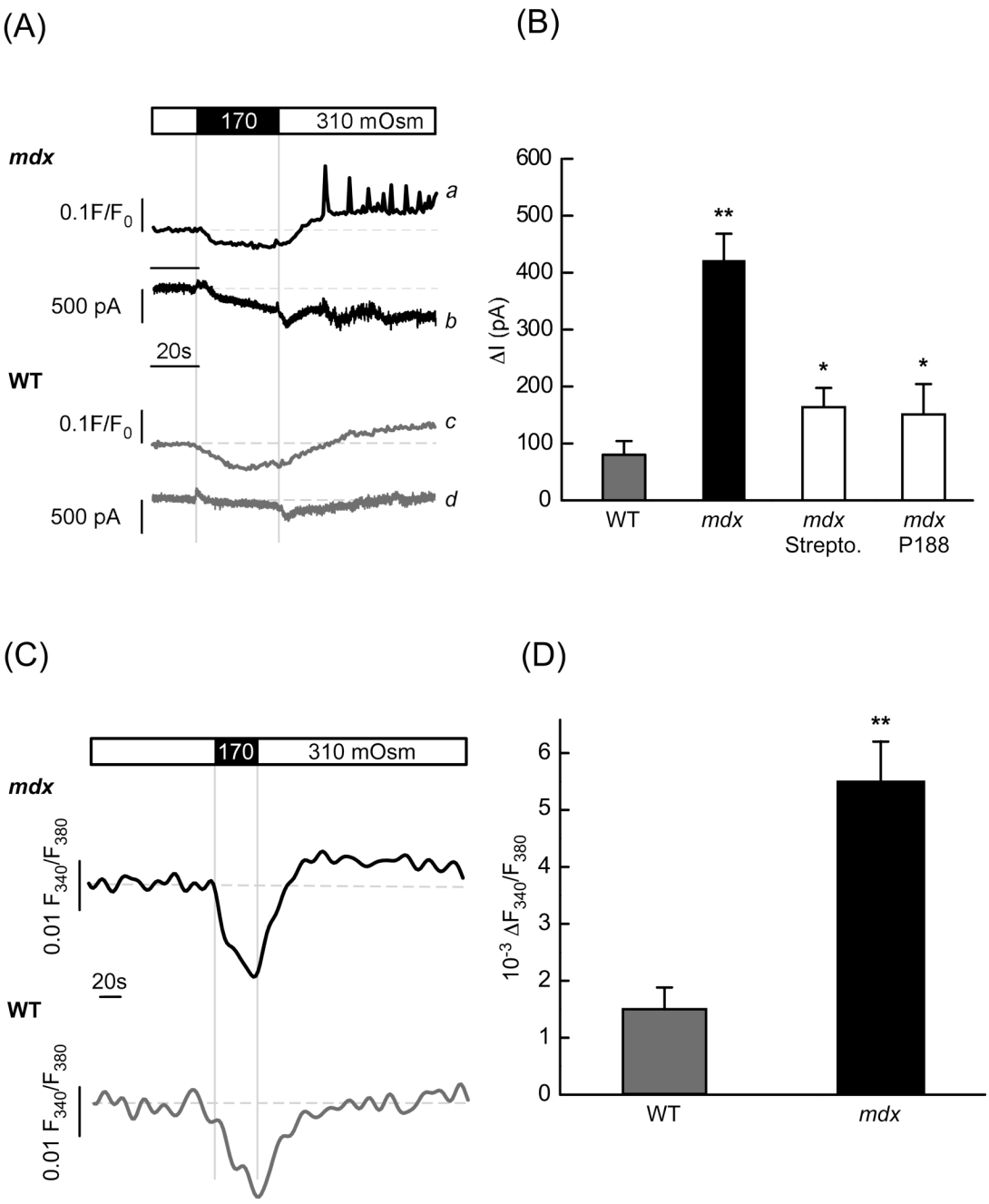

Fig. 4.

Stress-induced membrane currents and ion influxes. (*A*) Representative intracellular Ca^{2+} signals and ionic currents produced by stress in *mdx* (traces a and b) and WT (traces c and d) cardiac myocytes held at −70 mV. (*B*) Average increase of stress-induced inward currents in *mdx* and WT myocytes under control conditions (no inhibitors added) and in *mdx* cells treated with 100 μM streptomycin or 150 μM P-188 (n= 15, 18, 18, 11 for WT, *mdx*, P-188 and streptomycin, respectively). (*C*) Changes of intracellular Na^+ concentration elicited by osmotic swelling in *mdx* and in WT myocytes. (*D*) Relative changes in $[Na^+]_i$ in the WT and *mdx* cells determined at the end of the recording (between 110 s and 140 s after stress was applied, n=16 and 18, respectively).

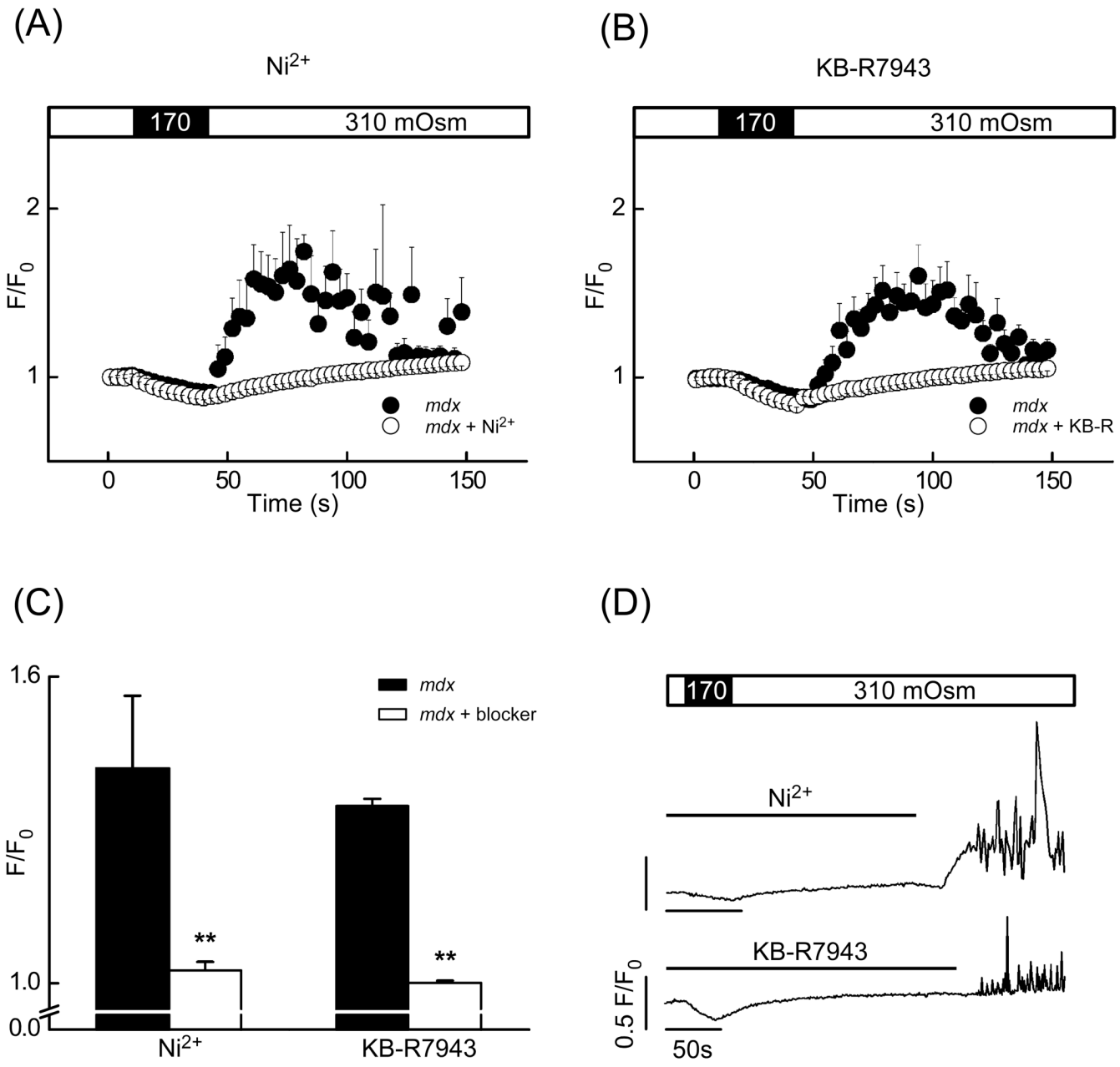

Fig. 5.

Ni^{2+} and KB-R7943: NCX-blockers significantly decreased the stress-induced Ca^{2+} signal amplitude. (*A*) and (*B*) Time-courses of normalized fluorescence intensity in *mdx* cardiomyocytes (black circles) and in *mdx* cardiomyocytes pretreated with an NCX inhibitor (white circles). (A) Presence of 5 mM Ni^{2+} or (*B*) 20 μM KB-R7943 during the stress. (*C*) Mean normalized fluorescence intensity after the stress in *mdx* myocytes under control conditions (black bar) and in the presence of an inhibitor (white bar; number of cells was n=5 and 15 for controls, n=11, 15 for Ni^{2+} and KB-R7943, respectively). (*D*) Sample traces of normalized Ca^{2+} signals appearing after the washout of 5 mM Ni^{2+} or 20 μM KB-R7943 as indicated by line bars.